

Source-tract coupling in birdsong production

Ezequiel M. Arneodo and Gabriel B. Mindlin

Department of Physics, FCEyN, UBA, Ciudad Universitaria, Pab I, Código Postal 1428, Buenos Aires, Argentina

(Received 2 March 2009; published 22 June 2009)

Birdsong is a complex phenomenon, generated by a nonlinear vocal device capable of displaying complex solutions even under simple physiological motor commands. Among the peripheral physical mechanisms responsible for the generation of complex sounds in songbirds, the understanding of the dynamics emerging from the interaction between the sound source and the upper vocal tract remains most elusive. In this work we study a highly dissipative limit of a simple sound source model interacting with a tract, mathematically described in terms of a delay differential equation. We explore the system numerically and, by means of reducing the problem to a phase equation, we are capable of studying its periodic solutions. Close in parameter space to the point where the resonances of the tract match the frequencies of the uncoupled source solutions, we find coexistence of periodic limit cycles. This hysteresis phenomenon allows us to interpret recently reported features found in the vocalization of some songbirds, in particular, “frequency jumps.”

DOI: [10.1103/PhysRevE.79.061921](https://doi.org/10.1103/PhysRevE.79.061921)

PACS number(s): 87.19.-j, 05.45.-a

I. INTRODUCTION

In the last years, birdsong has become a favorite animal model in which to explore the mechanisms involved in the learning of a complex behavior [1]. The reason is that almost forty percent of the known species of birds share with humans, and a few other examples in the animal kingdom, the need for a tutor in order to achieve the proper vocalizations of the adult [2]. This explains the particular interest that the neuroscience community has for this model.

In fact, much of the study of the animal behaviors that enhance the survival and reproduction of an individual has focused on their neural control. The generation of a behavior, however, involves strong interactions between the nervous system and a peripheral biomechanical system. This interaction is specially important in birdsong, where neural instructions drive a highly nonlinear physical system, the syrinx, capable of generating acoustic signals that range from simple whistles to complex sounds [3,4]. For this reason, it is important to understand the extent of the complexity that the syrinx is capable of, when driven by simple motor gestures. It is possible to obtain complex acoustic features with simple neural activity.

Despite the unique morphology of the avian vocal organ, the principal physical mechanism of sound generation shows striking parallels to that in the mammalian larynx [5,6]. More precisely, the basic mechanism of birdsong production resembles the generation of voiced sounds by humans: the expiratory airflow can drive sustained oscillations of the membranes (vocal folds in humans and labia in birds). The modulations produced in the airflow due to these tissue oscillations are responsible for the generation of sound. Between this sound source and the environment stands a tract. In humans, the dynamics of the oscillating vocal fold can be understood without taking into consideration the effect of the vocal tract (except in some exceptional situations [7,8]), which basically operates as a filter which enhances some frequencies of the sound signal generated by the source, and attenuates others. Yet, the air pressure between the labia, which provides the driving force responsible for their oscil-

latory behavior, depends on the pressure at the input of the vocal tract. For this reason, the filter, which modifies the pressure at the input of the tract, can in principle affect the labial motion. These source-tract interactions were shown to be capable of leading to sound instabilities [9].

In a model of a vocal organ capable of accounting for the generation of complex sounds, it is difficult to separate the complexity associated with the fact that the oscillating labia can display complex modal motion, from the phenomena strictly associated with the acoustic coupling between the sound sources and the tract [9]. For example, one of the most popular models used to represent the transfer of energy of an airflow to oscillatory tissue in voicing devices is known as the two-mass model. It was first introduced by Ishizaka and Flanagan [10] to account for the generation of voiced sounds by humans. It was thoroughly studied by a number of researchers [11,12], and (modulo small adaptations) assumes that the oscillating tissue can be described in terms of two masses. This model for the sound source was used to inspect the dynamics of a sound source, coupled to a tract [9]. This work shows that, in this model, complex behavior can emerge. Since the motion of an oscillating labium is described by a fourth-order dynamical system (position and velocity of the masses used to describe each part of the labia), complex dynamics might arise even if the coupling with the tract is neglected.

For this reason, we present a model which diminishes the complexity of the sound source dynamics to a minimum: without coupling, our model will only be capable of displaying periodic solutions. In this way, the phenomena associated with the sound source coupling will be easily identified. Moreover, working in a highly dissipative limit, we are capable of generating analytical expressions for the periodicity of the solutions found, which allows us to explore systematically the behavior of our system as different parameters are changed. In particular, we focus on the phenomenon known as “frequency jumps.” In this phenomenon, smooth changes in the system’s parameters lead to discontinuities of the sound’s fundamental frequency. This phenomenon is described by Zollinger *et al.* [13] as one of the three signatures

of nonlinearity in the sound source and reported experimentally in mockingbirds.

This work is organized as follows. In Sec. II, our model and a numerical exploration of its solutions are described. Section III deals with an analytical study of the model, reviewing a technique reported by Erneux *et al.* [14]. In Sec. IV we deal with the generation of synthetic sounds with our model of the avian vocal apparatus. Finally, we present our conclusions in Sec. V.

II. MODEL

Our model follows Titze's flapping model of fold oscillations during phonation [15]. The flapping model represents a good compromise between a realistic description and complexity, keeping the essentials of vocal fold physics. Without coupling, this model is mathematically described by a second-order dynamical equation. In order to study the mechanisms behind oscillations in the vocal folds, Titze proposed a simple model in which sustained oscillations arise whenever the energy transfer from the airflow to the folds overcomes the dissipative losses. This transfer can be achieved if the driving force exerted by the glottal pressure is larger when the folds are opening than when the folds are approaching each other. Titze observed that this requirement is met when the vocal folds assume an oscillation characterized by a "flapping" motion. This dynamics requires two active modes for each tissue: one consisting of a lateral motion and a second one which is an upward propagating wave. Assuming this distribution of active modes in the labia, one can write for x the midpoint position of a labium

$$\dot{x} = y$$

$$\dot{y} = -kx - \beta y - x^2 y + P_i + (P_{sub} - P_i)f(x, y),$$

where, in the second equation, the first term describes the elastic restitution of the labium, the second term represents dissipation, the third term a nonlinear saturation that bounds the labial motion, and finally, the last two terms account for the average interglottal pressure. This average pressure is described in terms of the subsyringeal pressure (P_{sub}), and the pressure of the tract (P_i). Assuming a simple geometry for the labial motion, Titze wrote $f(x, y)$ as a polynomial ratio. Let us explore in more detail the physical mechanisms at play in this model. To derive this result [15] the labia are assumed to support both lateral oscillations and an upward propagating surface wave. Hence, the opposing labia have a convergent profile when they move away from each other and a divergent profile when they move toward each other. In this way, a higher pressure is established between the labia during the opening phase, and an overall gain in energy during each cycle of oscillation. Physically what occurs is that while presenting a convergent profile, the average pressure between the labia is closer to the bronchial pressure, whereas interlabial pressure is closer to atmospheric pressure for a divergent profile. This results in a force in the same direction as the velocity of displacement of the labia, which might overcome the dissipation for high-enough values of the subsyringeal pressure. This qualitative argument lead us to ap-

proximate $f(x, y)$ by a term proportional to the velocity, i.e., $f(x, y) = y/v_{char}$, with v_{char} a characteristic velocity [16]. In this way, the interglottal pressure is capable of compensating the dissipation in the system, and transferring energy from the airflow into the labia. In a previous work [16], we explored dynamically the simplified model and studied its solutions as a function of the parameters (P_{sub}, k). The system presented the same qualitative behavior as the one reported in [17], where no simplifications were assumed beyond those presented in [15]. Moreover, the simplified model was used to synthesize the song of the *Zonotrichia capensis* in [16], and direct experimental support for it was reported in [19]. In this work ([19]), the simplified model was driven with time-dependent parameters $k(t)$ and $P_{sub}(t)$ whose time dependences were proportional to the recordings of ventral muscle activities and air sac pressure. Songs recorded simultaneously with the physiological activity were compared with the synthetic songs generated by the simplified model. The model was capable of generating recognizable songs.

Introducing that simple driving term $f(x, y) = y/v_{char}$, the system presents a fixed point at $(x, y) = (0, 0)$, and for certain values of the parameters a Hopf bifurcation will occur, by means of which the solutions become oscillatory (see Fig. 1 caption). After a change of scales, $t \rightarrow t/\gamma$ and $y \rightarrow \gamma y$, we write

$$\dot{x} = y \tag{1}$$

$$\dot{y} = -k\gamma^2 x + \gamma(P_{sub} - \beta)y - \gamma x^2 y + \gamma P_i(\gamma - y),$$

where $v_{char} = 1$ for the sake of simplicity. Beyond the Hopf bifurcation, the labia oscillate around their midpoint position. If $P_i \approx 0$, the dynamics of the source will be independent of the tract, and will consist only of these oscillations.

Additional nonlinear phenomena will occur when the interaction with the vocal tract is introduced. If the system interacts with a tube of length L , the suprasyringeal pressure P_i will be affected due to the feedback. This feedback will depend on the length of the tube and previous values of P_i itself. We compute the pressure at the input of the tube at time t as the result of two contributions: the one due to the glottal flow fluctuations being injected in the tube, and the other one corresponding to the backward propagating sound wave after the partial reflection at the distant end of the tube. The fluctuating glottal flow U_g induces velocity fluctuations in the air at the entrance of the tube $v = U_g/A_i$, where A_i is the tube's area [18]. These velocity fluctuations contribute to pressure fluctuations P_+ which can be written as $P_+ = \rho_0 c v = (\rho_0 c/A_i)U_g$ [20], where ρ_0 is the unperturbed air density and c stands for the sound speed. The average speed of the air through the glottis V_m can be estimated using a phenomenologically corrected version of Bernoulli's law as $V_m = \sqrt{\frac{2P_{sub}}{k_t \rho_0}}$ [15], where k_t stands for the transglottal pressure coefficient. Since the glottal area a_m is proportional to the midpoint departure of the labia x , approximating the flow by $U_g = V_m a_m$, we can write the contribution of the pressure at the input of the tract due to flow fluctuations as $P_+ = \alpha \sqrt{P_{sub}} x$, where α is inversely proportional to the area of the tube. If the tract is assumed to consist of a tube open at

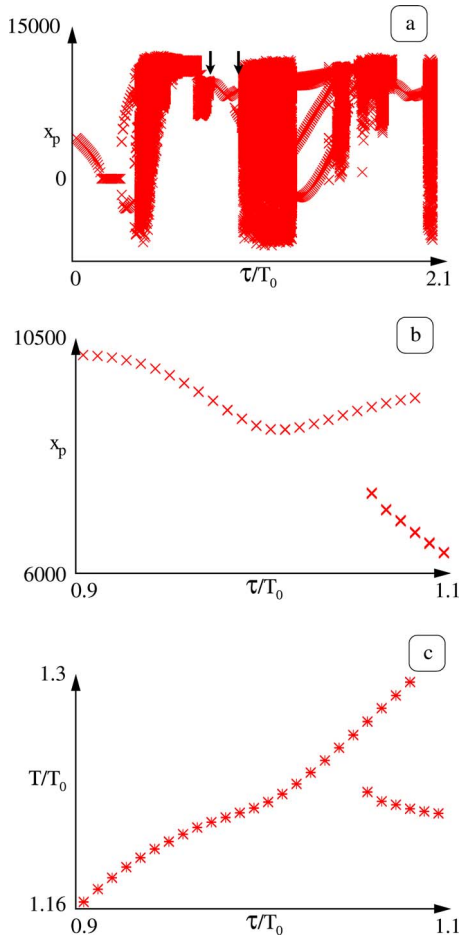


FIG. 1. (Color online) (a) Values of $x(t)$ at the intersection of trajectories in phase space (x, y) of system (1) with feedback (2) with the line $y=5000x$. (b) A detailed look at the section between the arrows suggests coexistence of solutions with different periods. (c) Measuring the periods T of trajectories in the detailed region for different initial conditions corroborates coexistence. For the parameters used for numerical integration, $(\gamma, \beta, P_{sub}, k) = (7000\pi, 0.1, 0.3, 1.0)$, and $P_{sub}=0.3$, the limit cycle found when $P_i=0$ has period $T_0=1/3500s$. When looking for coexistence of periodic solutions, $P_{sub}=0.3$ and feedback coefficients $(\alpha, r) = (1.0, 0.4)$.

the end opposed to the sound source, and the reflection coefficient is r [21], the total pressure at the input of the tract P_i can be written as

$$P_i(t) = \alpha\sqrt{P_{sub}}x - rP_i(t - \tau), \quad (2)$$

where $\tau = \frac{2L}{c}$ is the time it takes the sound wave to propagate to the far end of the tract and back at speed c . Numerical integration of the system with feedback (2) shows a variety of dynamical solutions. In particular, coexistence of periodic solutions is possible.

Recent work has shown that song is accompanied by a motor pattern responsible for the adjustment of the dimensions of the vocal tract based on the fundamental frequency generated by the syrinx [1,4,22]. For this reason, we restrained our numerical explorations of the model to those

parameters describing the tube in a way that $\tau = \frac{2L}{c}$ was of the same order of magnitude of the period of the solutions of the uncoupled syrinx T_0 . A first inspection of the solutions was conducted by means of numerically integrating the model for $\tau \in [0, \frac{5}{2}T_0]$. For each τ , system (1) with delayed feedback (2) was numerically integrated with different initial conditions and, after a transient, intersected with a Poincaré section in the (x, y) phase space. The intersection points x_p of the trajectories with the Poincaré section are plotted against τ in Fig. 1(a). A particularly interesting scenario occurs when τ is close to the period of the unperturbed limit cycle: coexistence of periodic solutions. This hysteresis between limit cycles is displayed in Fig. 1(b), which is an enlargement of the section between arrows of Fig. 1(a). In Fig. 1(c), the periods of numerically computed solutions in the detailed region are plotted. In fact, coexistence of periodic solutions is one of the key features displayed by limit cycle oscillators subject to delayed feedback [14,23]. Also, it is the one non-linear feature of our model on which we wish to focus. For that reason, we propose a simplified system that captures the dynamical mechanism and by yet can be treated analytically.

Notice that before coupling the source to the tube, the dynamics of the labia are driven by

$$\dot{x} = y \quad (3)$$

$$\dot{y} = -k\gamma^2x + \gamma(P_{sub} - \beta)y - \gamma x^2y,$$

which is the standard form of

$$\dot{u} = v - F(u) = v - \gamma u^3/3 + \gamma(P_{sub} - \beta)u \quad (4)$$

$$\dot{v} = -k\gamma^2u,$$

i.e., these two systems of equations are equivalent after writing $u=x$ and $v=\dot{x} - \gamma(P_{sub} - \beta)x + \gamma x^3/3$ [16]. The system of Eqs. (4) describes the dynamics of the Van der Pol oscillator; a paradigmatic model for relaxation oscillations. The cubic nullcline $v - F(u) = v - \gamma u^3/3 + \gamma(P_{sub} - \beta)u = 0$ is the key to understand the behavior of the system. Any trajectory in the (u, v) phase space rapidly zaps toward the nullcline, slowly crawls along it until an extremum is reached. After reaching this point, it zaps over the other branch of the nullcline. This is followed by another slow crawl until the second extremum is found where a new jumping off takes place, and the dynamics continues to repeat itself periodically. [24].

An equivalent dynamics takes place if the nullcline is approximated by straight lines,

$$f(u) = \begin{cases} u + 2\sqrt{P_{sub} - \beta} & x < -\sqrt{P_{sub} - \beta} \\ -u & |u| \leq \sqrt{P_{sub} - \beta} \\ u - 2\sqrt{P_{sub} - \beta} & x > \sqrt{P_{sub} - \beta}. \end{cases}$$

The relaxation oscillator presenting this nullcline, and the same time scale as our model obeys the following system of equations:

$$\dot{x} = y \quad (5)$$

$$\dot{y} = -k\gamma^2x + \gamma Sg\{[(P_{sub} - \beta) - x^2]\}y,$$

where $Sg(z)$ stands for *sign of z*: $Sg(z)=1$ if $z \geq 0$, $Sg(z)=-1$ otherwise. Using this model instead of Eq. (3) allows us to solve analytical expressions for the crawling along the nullcline, which will be advantageous in order to find analytical conditions for the phenomena we are interested in. Yet, it is worth pointing out that a nonlinear dissipation being turned on whenever the departure of x from equilibrium exceeds a threshold [as it is the case in the model described by Eq. (5)] is likely to be more realistic than the continuous nonlinear dissipation represented by the term $x^2\gamma$ in Eq. (3).

For these reasons, we are going to concentrate in the study of the dynamics of a source [whose autonomous dynamics is ruled by Eq. (5)] coupled to a simple tract, i.e., in the system ruled by

$$\ddot{x} + \nu Sg[x^2 - (P_{sub} - \beta)]\dot{x} + x = \delta(1 - \dot{x}/v_{char})[x - rx(t - \nu\tau)], \tag{6}$$

where $\gamma^2=1/k$ and $\nu=1/\gamma$ [25].

III. ANALYSIS OF THE MODEL

The advantage of working with Eq. (6) is that the free oscillator admits a simple solution: the evolution along the straight branches of the nullcline can be expressed analytically, and therefore the period of its periodic solution can be easily approximated: $T_0 \approx 2\nu \ln(3)$. The parameter ν scales the delay time of the feedback τ , as we wish to study how period changes with delays of the same order of magnitude. A technique used in [26] can be adapted to obtain a phase DDE, which will be analyzed in terms of the delay τ in the high dissipation, weak feedback case.

As mentioned in the previous section, Eq. (6) stands for a piecewise linear relaxation oscillator, subject to delayed feedback. The nature of its periodic solutions can be inspected analytically. We will begin by reviewing the unperturbed solutions ($\delta=0$). Afterward, a phase variable will be defined for the free oscillator and a method presented in [14] will be used to obtain a phase equation for the system when feedback is introduced. Out of this phase equation, conclusions can be drawn on how trajectories on the limit cycle are affected by the introduction of the feedback.

In the Liénard representation, the system represented by Eq. (6) takes the form of a system of two coupled first-order differential equations. Scaling time as $t \rightarrow t/\nu$, and choosing $P_{sub} - \beta = 1$ as a parameter consistent with oscillatory behavior, we arrive at

$$\epsilon u' = v - f(u) \tag{7}$$

$$v' = -u + \delta[1 - \nu[v - f(u)]]\{u - ru(t - \tau)\},$$

where $\epsilon=1/\nu^2$ and $f(u)$ is a piecewise linear function to result in $Sg(u^2-1)$ when derivated with respect to u ,

$$f(u) = \begin{cases} u+2 & u < -1 \\ -u & |u| \leq 1 \\ u-2 & u > 1. \end{cases}$$

In order to reach a definition for the phase of the free oscillator, we need to look at its limit cycle. We set $\delta=0$ in Eq. (7)

and find that with infinite dissipation ($\epsilon \rightarrow 0$), oscillations approach a discontinuous limit in which trajectories in (u, v) phase space satisfy

$$u_0(t) = \begin{cases} 3e^{-t} & 0 < t \leq t_0 \\ -3e^{-(t-t_0)} & t_0 < t \leq T_0, \end{cases}$$

$$v_0(t) = \begin{cases} u_0 - 2 & 0 < t \leq t_0 \\ u_0 + 2 & t_0 < t \leq T_0, \end{cases} \tag{8}$$

Here, $t_0 = \ln 3$ and $T_0 = 2t_0$ is the period of free oscillations. Equations (8) describe trajectories over two sections of the limit cycle of Eq. (7) when dissipation is high. When $u > 1$, the solution monotonically decreases along the right branch of the cycle, down to the point $(1, -1)$, where it jumps to the left branch, landing at $(-3, -1)$. Once there, it increases monotonically and departs from it at $(-1, 1)$, reaching the right branch at $(3, 1)$ and restarting the cycle. A phase can be defined that increases monotonically for the free oscillator. In this way, when the perturbation (the feedback) is turned on, since the amplitude of the periodic trajectories will remain almost unchanged, the way the motion is affected will be reflected by the dynamics of the phase variable [27]. Neglecting the time it takes trajectories to jump from one branch of the cycle to the other, the sought phase will grow uniformly as long as it satisfies

$$\frac{du_0}{d\phi} = -u_0. \tag{9}$$

The solutions of the system with feedback in the infinite dissipation limit ($\epsilon \rightarrow 0$) consist of a different parametrization in time of the nonperturbed limit cycle, i.e.

$$u = u_0[\phi(t)]. \tag{10}$$

When the feedback is introduced by setting $0 < \delta \ll 1$, an equation to account for the dynamics of the phase can be obtained. In first approximation, the orbit does not depend on δ , but changes in the phase may occur. For this infinite dissipation system, the Liénard representation with feedback, analogous to Eq. (7) takes the form

$$0 = v - f(u)$$

$$\dot{v} = -u + \delta[1 - \nu[v - f(u)]]\{u - ru(t - \tau)\}.$$

By elimination, it can be reduced to

$$\dot{u} = -u + \delta[u - ru(t - \tau)], \tag{11}$$

together with the conditions on the jumps between branches, namely, $u=-3$ if $u < 1$ and $u=3$ if $u > -1$. Using the definition of phase (10) and condition (9), DDE (11) can be written as

$$\frac{d\phi}{dt} = 1 - \delta + r\delta \frac{u_0[\phi(t - \tau)]}{u_0[\phi(t)]}.$$

In the search for a solution of this phase equation, we will use a perturbative procedure which takes into account the fact that there are two time scales in the problem [24]. A fast time t is adequate to describe the motion on the limit cycle of

the free oscillator. Due to the highly dissipative nature of the system, a much slower time $s = \delta t$ is required to describe the perturbations of the motion. In the *two-timing method*, the two time scales are treated as independent variables. In this way, we propose a perturbative solution $\phi(t, \delta) = \phi_0(t, s) + \delta\phi_1(t, s) + O(\delta^2)$. Derivation respect to time, following the chain rule, becomes $\frac{d}{dt} \rightarrow \frac{d}{dt} + \delta \frac{d}{ds}$. The zeroth-order equation reads $\frac{d\phi_0}{dt} = 1$, and its solution is

$$\phi_0(t, s) = 1 + \psi(s).$$

Using this result to go further to order δ , we are lead to equation

$$\frac{d\phi_1}{dt} = -1 - \frac{d\psi}{ds} + r \frac{u_0[t - \tau + \psi(s - \delta\tau)]}{u_0[t + \psi(s)]}.$$

Since $\phi_1(t, s)$ is the first-order correction to the phase perturbed by the feedback, we want its average respect to the fast time t over each period of oscillation to be zero. Otherwise the phase of the perturbed problem would diverge from the one of the free oscillation. This imposes the *solvability condition* $\frac{1}{T} \int_0^T \frac{d\phi_1}{dt} dt = 0$, or

$$\frac{d\psi}{ds} = -1 + rF(\Delta), \quad (12)$$

where

$$F(\Delta) = \frac{1}{T} \int_0^T \frac{u_0(s + \Delta)}{u_0(s)} ds,$$

and $\Delta = \psi(s - \delta\tau) - \psi(s) - \tau$ remains constant over the integral on $\varsigma = t + \psi(s)$. If we propose a linear solution for Eq. (12)

$$\psi(s) = \sigma s + \psi_0, \quad (13)$$

we find that

$$\Delta = -\tau(1 + \delta\sigma), \quad (14)$$

and $F(\Delta)$ can be computed. Note that in general, $F(\Delta)$ will take a different form depending on whether u_0 lies on the right or left branch of the limit cycle. In our problem,

$$F(\Delta) = (-1)^n e^{-\Delta - nt_0} \left[\left(\frac{4}{3}n + 1 \right) + \frac{4}{3}\Delta \right],$$

$$-(n+1)t_0 \leq \Delta < -nt_0,$$

with $n=0, 1, 2, \dots$. Plunging ansatz (13) into Eq. (12), we find an equation relating parameters σ and Δ ,

$$\sigma = -1 + rF(\Delta). \quad (15)$$

Together, expressions (14) and (15) lead to

$$\tau = \frac{-\Delta}{1 - \delta[1 - rF(\Delta)]}. \quad (16)$$

The period of the perturbed orbit is calculated as

$$T = \frac{2t_0}{1 + \delta\sigma} = \frac{2t_0}{1 - \delta[1 - rF(\Delta)]}, \quad (17)$$

with Δ satisfying Eq. (16). The way of computing the period of the solution for a given feedback strength δ and reflection

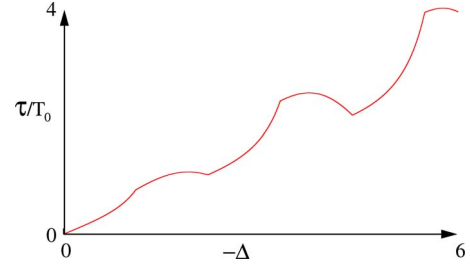


FIG. 2. (Color online) Solutions of Eq. (16) with $\delta=0.22$ and $r=0.7$. Every pair (Δ, τ) in the line is then used to calculate the period of a perturbed solution using Eq. (17). In this way, periodic solutions coexist when there are two points in the line with the same τ .

coefficient r consists in finding a solution of Eq. (16) [i.e., the values of (τ, Δ) that would satisfy the equation], and then introducing that Δ in the expression above. In Fig. 2 we plot a line of solutions of Eq. (16) for fixed δ and r . As it is, for some values of τ there are two values of Δ which satisfy the condition [that is, for some ranges of Δ the relation $\tau(\Delta)$ implied by Eq. (16) is noninjective]. In those cases, T admits two solutions.

The periods of the perturbed solutions T , computed as described above, are represented versus the delay τ with a solid line in Fig. 3. For that values of δ, r , periods of numerical solutions of system (7) are plotted as dots in the same graph to illustrate the agreement of the analytical calculations with the numerical solution (see caption of Fig. 3 for the parameters used in the simulation). The period exhibits bistability for τ sufficiently large. When a bistability region is crossed, a “jump” occurs in T .

IV. ACOUSTIC FEATURES OF THE SOLUTIONS

The jumps in periods of solutions mentioned in the previous section bear a resemblance to the frequency jumps discussed in Sec. II. This nonlinear feature of systems with delayed feedback is one of the candidates for being responsible for the generation of the phenomenon. By synchronizing an adequate pressure gesture with an excursion of parameter τ which includes the crossing of a coexistence region,

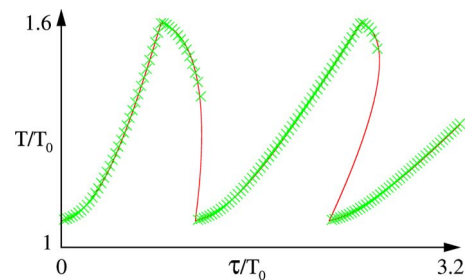


FIG. 3. (Color online) Period as a function of delay τ for DDE system (6) with $\delta=0.22$, $r=0.7$. The line is the plot of the analytical result obtained by means of the two-time method on the phase equation of the system. The dots correspond to period measurements on numerical solutions of Eq. (7) (in the limit $\epsilon \rightarrow 0$; $\nu = 100$ was set).

we expect to generate a synthetic syllable in which a frequency jump occurs. A set of equations similar to Eq. (1) has been previously used to generate diverse syllables, as pressure P_{sub} was varied over a time interval following different patterns [28]. Here, we will introduce a very simple pressure pattern, which consists of increasing the pressure beyond the value for which the folds oscillate, and after a time interval, returning to a subthreshold value, at which the folds stay in a stable fixed point (no displacement). During that time, the length of the tract L is linearly incremented, inducing the delay τ to cross a region of bistability. As a consequence, a jump will occur in the period of the solutions. This effect is reflected by the acoustic features of the synthetic syllable. A jump in the frequency of the generated sound occurs, as expected, when the periodic solution corresponding to the starting length L_i no longer exists, and trajectories in the phase space are attracted to the periodic orbit corresponding to final length L_f . Figure 4 illustrates, from top to bottom, the sonogram of the synthesized sound, the normalized sound wave, the pressure gesture, and the vocal tract stretching.

Not every jump in the fundamental frequency of a bird-song can be attributed to this mechanism. In some cases, jumps correspond to sounds generated successively by each of the two sound sources. Yet, unilaterally generated sounds with frequency jumps have been recently reported [13]. The mechanism illustrated in this work shows that in these cases, rapid acoustic changes do not necessarily require fast muscle control.

V. CONCLUSIONS

In this work we studied the dynamical responses of a simple interacting sound source-vocal tract system. We have shown that for lengths such that the resonances are similar to the natural frequency of the source, multistability occurs. This dynamical scenario implies that it is possible to have rapid changes in the acoustic output of the system, even under smooth variations of the parameters.

As it was mentioned upon introduction of the model in Sec. II, the dynamical system accounting for the avian vocal organ presents little complexity, namely, just the possibility to go through a Hopf bifurcation. It is therefore the interaction of the vocal tract which is responsible for the nonlinear effect reflected by the frequency jump in the syllable.

Complex behavior arises when the tract is taken into consideration. In our model, the vocal tract does not act as a mere filter that enhances some frequencies and attenuates others [28], but it interacts with the tract, inducing a delayed feedback in the supraglottal pressure P_i . Recent observations suggest that by varying the geometry of the vocal tract, a feedback in supraglottal pressure is allowed (see, for instance, Hatzikirou *et al.*, [9]). Among the complex bifurcation scenarios led to by introducing the interaction with the tract, delayed feedback appears as a candidate for the production of the jumps in pitch mentioned in the reference. The use of the minimal model for the syrinx proposed in this paper only pursued the goal of identifying what part of the complexity of the syllable has origin in the complexity of the vocal organ, and which comes as a signature of nonlinear effects introduced by the interaction with the tract (such as

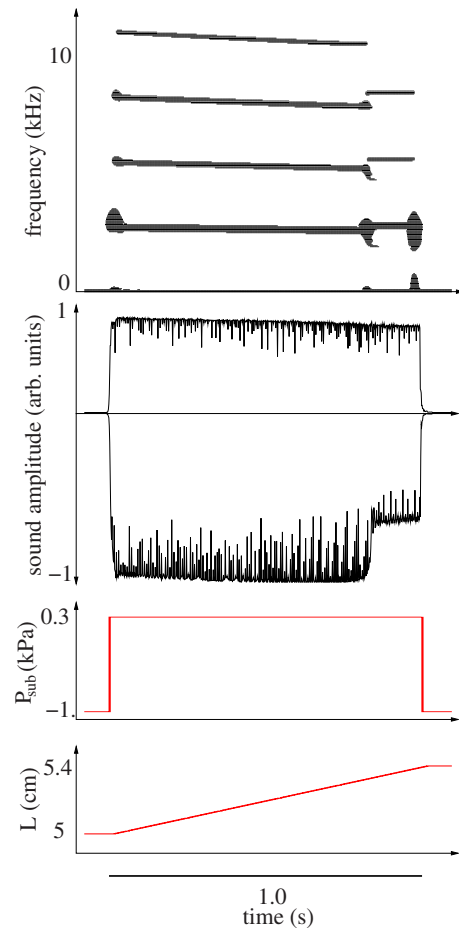


FIG. 4. (Color online) Synthetic sound produced by numerical integration of Eqs. (1) and (2). Sound (second panel from top) is produced when the system is driven by a simple pressure gesture (third panel from top). As the longitude of the tract is varied within the region of coexistence (bottom panel), the sonogram (top panel) exhibits a frequency jump. The system was integrated with parameter values $(\gamma, \beta, P_{sub}, k) = (7000\pi, 0.1, 0.3, 1.0)$, and $P_{sub} = -1.0$, and feedback coefficients $(\alpha, r) = (1.0, 0.4)$ to produce the syllable ($P_{sub} = -1.0$ corresponds to no phonation), and L grew linearly during phonation from $L_i = 5.01$ cm to $L_f = 5.4$ cm, corresponding to delays $\tau_i = 29.48$ ms and $\tau_f = 31.75$ ms.

coexistence of periodic solutions). When the frequency associated with the delay is not close to the fundamental frequency of the sound produced, the vocal tract introduces no nonlinear effect. Once settled this issue, the mechanism is easily applicable to more complete models including more complex neuromuscular patterns as well as a more detailed level of description of the syrinx.

Birdsong production requires the integration of a nervous system to peripheral biomechanical systems. In general, the task of unveiling where complexity is originated is not an easy one. This issue is addressed by Zollinger *et al.* in [13], where they suggest that nonlinear phenomena may not require active neural control, but could as well arise from nonlinear effects occurring in the periphery. From a wider perspective, this mechanism highlights the need to study in parallel neural control and the dynamics of the periphery in order to understand the emergence of complex behavior.

- [1] P. Zeigler and P. Marler, *Neuroscience of Birdsong* (Cambridge University Press, Cambridge, Massachusetts, 2004).
- [2] A. J. Doupe and P. K. Kuhl, *Annu. Rev. Neurosci.* **22**, 567 (1999).
- [3] M. S. Fee, B. Shraiman, B. Pesaran, and P. P. Mitra, *Nature* (London) **395**, 67 (1998).
- [4] R. A. Suthers and D. Margoliash, *Curr. Opin. Neurobiol.* **12**, 684 (2002).
- [5] F. Goller and O. N. Larsen, *Proc. Natl. Acad. Sci. U.S.A.* **94**, 14787 (1997).
- [6] O. N. Larsen and F. Gollerf, *Proc. R. Soc. London, Ser. B* **266**, 1609 (1999).
- [7] I. Titze, T. Riede, and P. Popolo, *J. Acoust. Soc. Am.* **123**, 1902 (2008).
- [8] I. R. Titze, *J. Acoust. Soc. Am.* **123**, 2733 (2008).
- [9] H. Hatzikirou, W. T. Fitch, and H. Herzel, *Acta. Acust. Acust.* **92**, 468 (2006).
- [10] K. Ishizaka and J. Flanagan, *Synthesis of Voiced Sounds From a Two-Mass Model of the Vocal Chords* (Dowden, Hutchinson, and Ross, Strousburg, 1973).
- [11] H. Herzel, D. Berry, I. Titze, and I. Steinecke, *Chaos* **5**, 30 (1995).
- [12] X. Pelorson, A. Hirschberg, R. R. van Hassel, A. P. J. Wijnands, and Y. Auregan, *J. Acoust. Soc. Am.* **96**, 3416 (1994).
- [13] S. A. Zollinger, T. Riede, and R. A. Suthers, *J. Exp. Biol.* **211**, 1978 (2008).
- [14] T. Erneux and J. Grasman, *Phys. Rev. E* **78**, 026209 (2008).
- [15] I. R. Titze, *J. Acoust. Soc. Am.* **83**, 1536 (1988).
- [16] R. Laje, T. J. Gardner, and G. B. Mindlin, *Phys. Rev. E* **65**, 051921 (2002).
- [17] T. J. Gardner, G. A. Cecchi, M. O. Magnasco, R. Laje, and G. B. Mindlin, *Phys. Rev. Lett.* **87**, 208101 (2001).
- [18] This expression is valid as long as the period of the flow fluctuations at the sound source is large compared to the time it would take a density perturbation to span the transversal area of the tube connected to the tube, which can be approximated by $\sqrt{A_i}/c$, where c stands for sound speed. For flow fluctuations of the order of the KHz, and transversal areas in the millimeters, this condition is satisfied.
- [19] G. B. Mindlin, T. J. Gardner, F. Goller, and R. Suthers, *Phys. Rev. E* **68**, 041908 (2003).
- [20] B. H. Story and I. Titze, *J. Acoust. Soc. Am.* **97**, 1249 (1995).
- [21] A monotonically decreasing $r=r(L)$ can be used to account for losses of the sound waves in the tube, which are neglected in this work.
- [22] T. Riede, R. A. Suthers, N. H. Fletcher, and W. E. Blevins, *Proc. Natl. Acad. Sci. U.S.A.* **103**, 5543 (2006).
- [23] C. Beta, M. Bertram, A. S. Mikhailov, H. H. Rotermund, and G. Ertl, *Phys. Rev. E* **67**, 046224 (2003).
- [24] S. H. Strogatz, *Nonlinear Dynamics and Chaos* (Perseus, Cambridge, Massachusetts, 2000).
- [25] The right-hand side of Eq. (5) is a first-order approximation of Eq. (2) for $r < 1$. That is, the first term in the rightmost part of $P_i(t) = \alpha\sqrt{P_{sub}}x - rP_i(t-\tau) \approx \alpha\sqrt{P_{sub}}[x(t) - rx(t-\tau)] + r^2P_i(t-2\tau) + \dots$. In Eq. (5), we also name $\delta = \alpha\sqrt{P_{sub}}$.
- [26] J. Grasman, *Asymptotic Methods for Relaxation Oscillations and Applications* (Springer-Verlag, New York, 1987).
- [27] A. Pikovsky, M. Rosenblum, and J. Kurths, *Synchronization, A Universal Concept in Nonlinear Sciences* (Cambridge University of Postdam, Germany, 2001).
- [28] G. Mindlin and R. Laje, *The Physics of Birdsong* (Springer, New York, 2005).